

Precessional dynamics of black hole triples: binary mergers with near-zero effective spin

Fabio Antonini,^{1,*} Carl L. Rodriguez,² Cristobal Petrovich,³ and Caitlin L. Fischer²

¹*Center for Interdisciplinary Exploration and Research in Astrophysics (CIERA) and Dept. of Physics and Astronomy, Northwestern University, 2145 Sheridan Rd, Evanston, IL 60208, USA*

²*MIT-Kavli Institute for Astrophysics and Space Research, 77 Massachusetts Avenue, 37-664H, Cambridge, MA 02139, USA*

³*Canadian Institute for Theoretical Astrophysics, University of Toronto, 60 St George Street, ON M5S 3H8, Canada*

(Dated: December 14, 2024)

The binary black hole mergers detected by Advanced LIGO/Virgo have shown no evidence of large black hole spins. However, because LIGO/Virgo best measures the effective combination of the two spins along the orbital angular momentum (χ_{eff}), it is difficult to distinguish between binaries with slowly-spinning black holes and binaries with spins lying in the orbital plane. Here, we study the spin dynamics for binaries with a third black hole companion, and identify a new dynamical process which preferentially leads to binary black hole mergers with small χ_{eff} . While the binary undergoes fast Lidov-Kozai oscillations, the two black hole spins slowly rotate onto the plane perpendicular to the total angular momentum of the triple. For spins initially aligned with the orbital angular momentum of the binary, the differential rotation of the spin vectors onto a fixed plane causes χ_{eff} to “freeze” near zero as the orbit decays through the emission of gravitational waves. Through a population study, we show that this effect predominantly produces binaries with near-zero χ_{eff} even for maximally-spinning black holes. We conclude that such triples could provide a natural explanation for the low χ_{eff} values of the binary black hole mergers without the need to invoke unrealistically small black hole spins.

I. INTRODUCTION

Since the first detection of merging black hole (BH) binaries, there has been a proliferation of astrophysical models for producing such systems. To narrow the range of possibilities, it has been shown that the misalignment between the binary’s orbital angular momentum and the BH spins can serve as an important discriminant between these different formation channels (e.g., [1–3]). Here, we consider binary BH mergers formed through the evolution of stellar triples in the field. In this scenario, the binary is driven to merger by the presence of a third BH companion. This dynamical configuration can induce high eccentricities in the inner BH binary via the Lidov-Kozai (LK) mechanism [4, 5], eliminating the need for the common-envelope phase often invoked in standard binary evolution models [6–8]. We specifically consider the secular evolution of the effective spin parameter, χ_{eff} (see Eq. 4), the combination of BH spins best measured by current gravitational-wave (GW) detectors [9–11].

To date, the BH binaries detected by LIGO/VIRGO have all exhibited small χ_{eff} , with all but one—GW151226—being consistent with $\chi_{\text{eff}} = 0$ [10–13]. The individual component spins in isolated field binaries are expected to be nearly perpendicular to the binary orbital plane [14], meaning that current measurements would imply slow rotation of the BHs (if these are formed in the field [15]). Low spins, however, are in contrast with

current observational constraints and theoretical expectations, both favoring rapid BH rotation at formation [16, 17]. In this letter, we show that a more consistent explanation is possible: the small values of χ_{eff} are a consequence of the spin-orbit tilt produced by the binary’s long-term interaction with a distant companion.

In what follows, unless otherwise specified, we work under the assumption that the BH spin vectors are initially nearly aligned with the inner binary angular momentum. Spin-orbit alignment is generally observed in solitary (solar-type) binaries with relatively large separation ($\lesssim 40\text{AU}$; [18]) and could either be primordial in origin ([19]) or produced through tidal evolution and mass transfer during stellar evolution prior to BH formation [e.g., 14].

II. ORBIT-AVERAGED EQUATIONS

We consider a BH binary with total mass $M = m_1 + m_2$, semi-major axis a and eccentricity e , orbited by a tertiary BH with mass m_3 on an outer orbit with semi-major axis a_{out} and eccentricity e_{out} . We work in terms of the dimensionless inner-orbit angular-momentum vector, $\mathbf{j} = \sqrt{1 - e^2}\hat{\mathbf{j}}$, and the eccentricity vector, $\mathbf{e} = e\hat{\mathbf{e}}$, defined in Jacobi coordinates. We define the circular angular momenta for the inner and outer orbits as $L = \mu\sqrt{GMa}$ and $L_{\text{out}} = \mu_{\text{out}}\sqrt{G(M + m_3)a_{\text{out}}}$ respectively, with $\mu = m_1m_2/M$, and $\mu_{\text{out}} = Mm_3/(M + m_3)$. Finally, the total angular momentum of the triple system is $\mathbf{J} = L\mathbf{j} + L_{\text{out}}\mathbf{j}_{\text{out}}$, where \mathbf{j}_{out} is the outer-orbit angular-momentum vector. In the absence of dissipation

* fabio.antonini@northwestern.edu

(e.g. gravitational waves), \mathbf{J} is constant, and is normal to the “invariable plane” of the triple.

A tertiary companion inclined with respect to the binary orbit by an angle, denoted by I , in the approximate range $[40, 140^\circ]$ induces periodic LK oscillations in the inner binary eccentricity and inclination. We describe this evolution using the secular equations at the octupole level of approximation (Eq. 17-20 in [20], see also [21]) The associated timescale of the LK oscillations is [e.g., 22]

$$t_{\text{LK}} = \frac{1}{\nu} \left(\frac{M}{m_3} \right) \left(\frac{a_{\text{out}} j_{\text{out}}}{a} \right)^3, \quad (1)$$

with $\nu = \sqrt{GM/a^3}$. We add 1 and 2.5 post-Newtonian (pN) terms to the standard LK equations, describing the (Schwarzschild) precession of the argument of periapsis and the orbital decay due to gravitational-wave emission respectively [e.g., 23]. We also add the spin-orbit interaction terms [e.g., 24]:

$$\frac{d\mathbf{S}_1}{dt} \Big|_{\text{SO}} = \frac{2GL}{c^2 a^3 (1-e^2)^{3/2}} \left(1 + \frac{3m_2}{4m_1} \right) \mathbf{j} \times \mathbf{S}_1 \quad (2)$$

$$\frac{d\mathbf{S}_2}{dt} \Big|_{\text{SO}} = \frac{2GL}{c^2 a^3 (1-e^2)^{3/2}} \left(1 + \frac{3m_1}{4m_2} \right) \mathbf{j} \times \mathbf{S}_2, \quad (3)$$

where \mathbf{S}_1 and \mathbf{S}_2 are the spins of m_1 and m_2 respectively. The spin vectors can also be written in terms of the dimensionless spin parameter χ as $\mathbf{S}_{1(2)} = \chi_{1(2)} G m_{1(2)}^2 / c$, with $|\chi_{1(2)}| \leq 1$. The total spin vector is then given as $\mathbf{S} = \mathbf{S}_1 + \mathbf{S}_2$.

In what follows we will often refer to the evolution of the misalignment between the total or component spins and the inner-orbit angular momentum using $\theta = \cos^{-1} \hat{\mathbf{S}} \cdot \hat{\mathbf{j}}$ or $\theta_{1(2)} = \cos^{-1} \hat{\mathbf{S}}_{1(2)} \cdot \hat{\mathbf{j}}$. Similarly, the misalignment between the spins and the total angular momentum of the triple is given by $\Theta_{1(2)} = \cos^{-1} \hat{\mathbf{S}}_{1(2)} \cdot \hat{\mathbf{J}}$. Finally, we define the binary effective spin parameter as

$$\chi_{\text{eff}} = \frac{(m_1 \chi_1 \cos \theta_1 + m_2 \chi_2 \cos \theta_2)}{M}. \quad (4)$$

III. SECULAR SPIN-ORBIT DYNAMICS

To the lowest pN order, each of the two BH spin vectors precess in response to torques from the binary at the orbit-averaged rate [e.g., 25]:

$$\Omega_{\mathbf{S}_{1(2)}} = \frac{2G\mu}{c^2 a (1-e^2)} \left(1 + \frac{3m_{2(1)}}{4m_{1(2)}} \right) \nu. \quad (5)$$

For fixed \mathbf{j} , the precession described by Equations (2)-(3) has the form of uniform precession of the spin vector about the binary angular momentum vector. At the same time, during the LK oscillations, the binary angular momentum vector precesses around the total angular momentum of the triple system at a characteristic rate: $\Omega_{\text{LK}} \approx t_{\text{LK}}^{-1}$.

We define the adiabaticity parameter:

$$R_{1(2)} \equiv \left| \frac{\Omega_{\mathbf{S}_{1(2)}}}{\Omega_{\text{LK}}} \right|_{e=0} = 2 \frac{G\mu}{c^2 a} \left(1 + \frac{3m_{2(1)}}{4m_{1(2)}} \right) \nu t_{\text{LK}}. \quad (6)$$

There are three possible regimes for the evolution of each of the two BH spins [26–28]: (i) for $R_{1(2)} \gg 1$ (adiabatic regime), the spin follows $\hat{\mathbf{j}}$ adiabatically, maintaining an approximately constant spin-orbit alignment angle $\theta_{1(2)}$ and consequently a constant χ_{eff} ; (ii) for $R_{1(2)} \ll 1$ (non-adiabatic regime), $\hat{\mathbf{S}}_{1(2)}$ effectively precesses about $\hat{\mathbf{J}}$, maintaining an approximately constant angle $\Theta_{1(2)}$; and (iii) for $R_{1(2)} \approx 1$ (trans-adiabatic regime), the spin precession rate matches the orbital precession rate and the evolution of the spin orbit orientation can become more complicated.

We might expect that at $R \approx 1$ the spin-orbit angle will exhibit chaotic evolution due to overlapping resonances, possibly leading to a wide range of final spin-orbit angles. In reality, we find that such chaotic behavior is suppressed in most cases. The main reason for this is that when $R \approx 1$, the 1pN apsidal precession rate of the inner binary orbit matches Ω_{LK} . In this situation, the LK oscillations are quenched [23] and only modest spin-orbit misalignments can be induced [28]. This indicates (and the numerical simulations below confirm) that the non-adiabatic regime is the most relevant for merging BHs. Only when $R \ll 1$ does the spin-orbit orientation change significantly while the binary simultaneously experiences extreme eccentricity excitation that can lead to its coalescence through energy loss by GW radiation.

A. Differential spin precession and freezing of χ_{eff}

For non-adiabatic systems, the spins of the BHs will precess about the total angular momentum \mathbf{J} of the triple [e.g., 26]. Because a system must have an initial inclination $I \approx \pi/2$ in order to reach $e \sim 1$ [e.g., 8], and because by assumption the BH spins are initially nearly aligned with \mathbf{j} , the spin vectors will appear to effectively rotate onto the invariable plane. This implies that $\Theta_{1(2)} \simeq \text{const} \approx \pi/2$ throughout the evolution.

If the two inner bodies were of exactly the same mass, then their spins would precess by the same amount and remain aligned ($\theta = \theta_1 = \theta_2$). However, as $m_1 \neq m_2$ more generally, $\hat{\mathbf{S}}_1$ and $\hat{\mathbf{S}}_2$ rotate onto the invariable plane (i.e., $\hat{\mathbf{S}}_{1(2)} \cdot \mathbf{J} = 0$) at different rates. We quantify this using the differential precession timescale, which is approximated by the expression:

$$\tau_{\text{rp}} \equiv 2\pi / |\Omega_{S_1} - \Omega_{S_2}| \simeq K \frac{c^2 a}{G\mu} \frac{m_1 m_2}{|m_2^2 - m_1^2|} \frac{1}{\nu}, \quad (7)$$

where $K = 0.3$ is calibrated from numerical simulations and reproduces numerical results within a small factor. Two situations, considered below, occur depending on

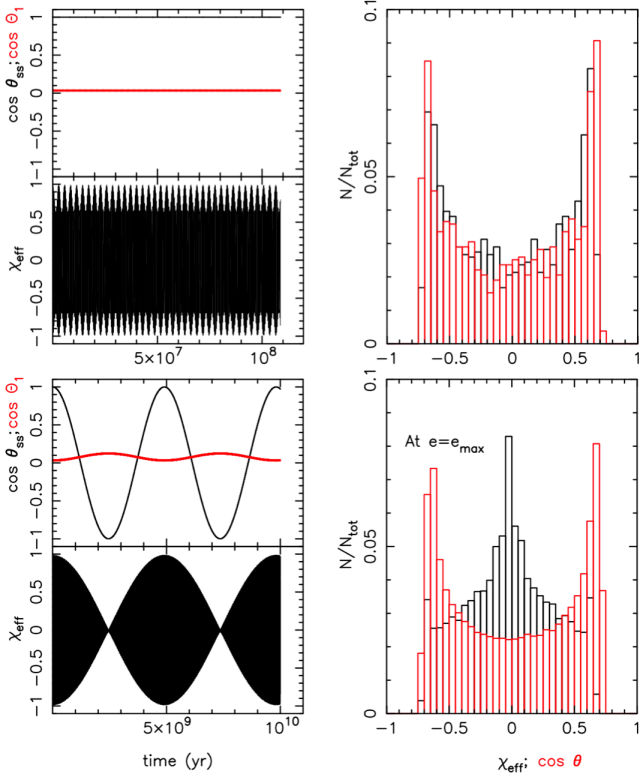


FIG. 1. Evolution of a system undergoing prominent LK oscillations. The initial conditions in the top and bottom set of panels are the same. However, in the bottom set of panels we allow the system to evolve for a longer time so that a larger phase difference between the two spin vectors can emerge. The right panels show the distribution of χ_{eff} and $\cos \theta$ at the moment e reaches its maximum during the LK oscillations. When the two spins become anti-aligned, $\cos \theta_{\text{ss}} = -1$ and $\chi_{\text{eff}} \approx 0$, skewing the distribution of χ_{eff} towards zero. The initial conditions are $\chi_1 = \chi_2 = 1$, $m_1 = 19.9M_{\odot}$, $m_2 = 20.3M_{\odot}$, $m_3 = 20.1M_{\odot}$, $a = 18\text{AU}$, $a_{\text{out}} = 577\text{AU}$, $e = 0.33$, $e_{\text{out}} = 0.64$ and $I = 95.4^{\circ}$. (For illustrative purposes, we did not include the dissipative 2.5pN terms in this example.)

whether the spins of the BHs experience significant precession before a time τ_m at which the binary evolution is halted (e.g., due to merger induced by GW radiation).

If $\tau_{\text{rp}} \gg \tau_m$, then the precession of the spin vectors is unimportant as their relative orientation remains unchanged over time. For these systems

$$\chi_{\text{eff}} = \frac{m_1\chi_1 + m_2\chi_2}{M} \cos \theta = \frac{m_1\chi_1 + m_2\chi_2}{M} \hat{\mathbf{S}} \cdot \hat{\mathbf{j}}. \quad (8)$$

We define a fixed reference frame with $\hat{\mathbf{z}} = \hat{\mathbf{J}}$. Assuming the quadrupole test-particle approximation, we have that $\hat{\mathbf{j}} = \sqrt{2/5} \cos \Omega \hat{\mathbf{x}} + \sqrt{2/5} \sin \Omega \hat{\mathbf{y}} \pm \sqrt{3/5} \hat{\mathbf{z}}$ at the maximum eccentricity, e_{max} , reached during a LK cycle with positive $\hat{\mathbf{z}}$ orientation for initially prograde systems. Since $R \ll 1$, we can consider $\hat{\mathbf{S}}$ to be fixed in the $\hat{\mathbf{x}} - \hat{\mathbf{y}}$ plane ($\hat{\mathbf{S}} = \hat{\mathbf{x}}$ without loss of generality), implying that $\hat{\mathbf{S}} \cdot \hat{\mathbf{j}} = \sqrt{2/5} \cos(\Omega_{\text{LK}}t)$. The time averaged distribution

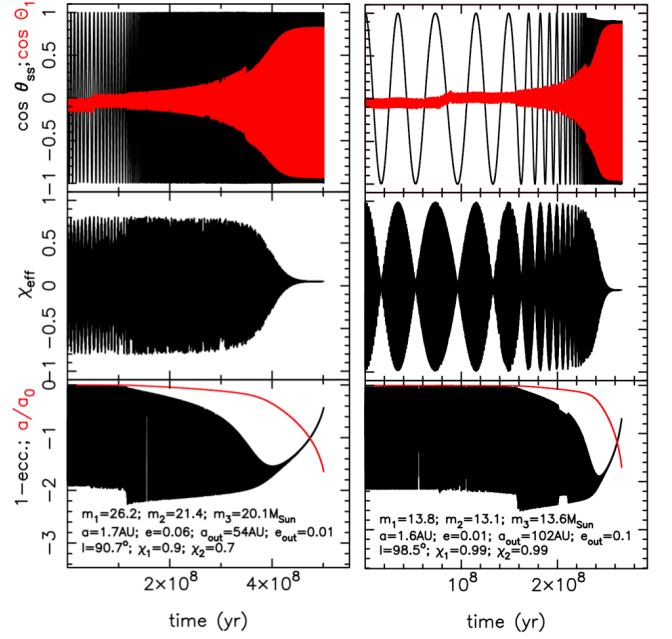


FIG. 2. Example cases of merging systems that evolve in the regime $\tau_{\text{rp}} < \tau_m$. As the system eccentricity and semi-major axis decrease due to the dissipative 2.5pN terms, the range of allowed values for χ_{eff} tends to evolve towards zero. Corresponding initial parameters are given in the lower panels.

of χ_{eff} at $e = e_{\text{max}}$ simply becomes

$$n_{\chi_{\text{eff}}} = \frac{1}{\pi C \left(2/5 - [\chi_{\text{eff}}/C]^2 \right)^{1/2}}. \quad (9)$$

where $C = (m_1\chi_1 + m_2\chi_2)/M$. An example case is illustrated in the upper panels of Figure 1. The angle between the two spin vectors ($\cos \theta_{\text{ss}} = \hat{\mathbf{S}}_1 \cdot \hat{\mathbf{S}}_2$) and $\cos \Theta_1$ are both constant. The distribution of χ_{eff} at $e = e_{\text{max}}$ is nearly identical to the distribution of $\cos \theta$ and, as expected, peaks at $\approx \pm\sqrt{2/5} = \pm 0.63$.

If $\tau_{\text{rp}} \lesssim \tau_m$, the differential precession of the two spins plays a key role in determining the evolution of χ_{eff} over time. In this case, we find that a new dynamical process arises which drives χ_{eff} towards zero after a timescale τ_{rp} . An example is shown in the bottom panels of Figure 1. The initial conditions are the same in both panels of Figure 1, but the system in the bottom panels was integrated for longer so that the spin vectors could precess by a large angle. By comparing the evolution of χ_{eff} in the lower left panel to the solid line in the upper left panel, we see that χ_{eff} progressively clusters around zero as the two spin vectors become anti-aligned at $\cos \theta_{\text{ss}} = -1$. During the evolution, $\cos \Theta_1$ remains nearly constant, indicating that the spins are confined to rotate within the invariable plane of the triple. Clearly, it is the differential precession of the two BH spins that drives the distribution of χ_{eff} to near-zero values. While the two spin vectors precess away from each other onto a fixed plane, their sum

decreases, causing χ_{eff} to also decrease. As long as the two BHs have similar spin magnitudes and masses, Eq. (4) implies that $\chi_{\text{eff}} \approx 0$ when the two spin vectors have rotated by 180° from each other (i.e., at $\cos \theta_{\text{ss}} = -1$).

The bottom right panel of Figure 1 shows the distribution of χ_{eff} and θ at the moment $e = e_{\text{max}}$ for the inner binary. Because the spin vectors are no longer aligned with each other, the distribution of χ_{eff} is now different from the distribution of $\cos \theta$, and peaks near zero. We can analytically approximate this distribution. The binary χ_{eff} is the sum of two contributions $\psi_{1(2)} = m_{1(2)}\chi_{1(2)}\cos\theta_{1(2)}/M$ which, at the maximum eccentricity, have the independent distributions:

$$n_{1(2)} = \frac{1}{\pi C_{1(2)} \left(2/5 - [\psi_{1(2)}/C_{1(2)}]^2\right)^{1/2}}, \quad (10)$$

with $C_{1(2)} = m_{1(2)}\chi_{1(2)}/M$. Thus, the time averaged distribution of χ_{eff} at $e = e_{\text{max}}$ after a time $\gtrsim \tau_{\text{rp}}$ becomes

$$n_{\chi_{\text{eff}}} = n_1 \otimes n_2 = \frac{1}{C_2 C_1 \pi^2} \times \int du \frac{H\left(2/5 - \left[\frac{u}{C_1}\right]^2\right)}{\left(2/5 - \left[\frac{u}{C_1}\right]^2\right)^{1/2}} \frac{H\left(2/5 - \left[\frac{\chi_{\text{eff}} - u}{C_2}\right]^2\right)}{\left(2/5 - \left[\frac{\chi_{\text{eff}} - u}{C_2}\right]^2\right)^{1/2}}, \quad (11)$$

where $H(\cdot)$ is the Heaviside function.

In Figure 2 we show example merging BH systems for which τ_{rp} (calculated at time zero) is significantly shorter than the binary merger time. Because the differential precession of the two BH spins skews the distribution of χ_{eff} towards zero, χ_{eff} evolves and tends to “freeze” near zero as the binary eccentricity and semi-major axis damp due to the 2.5pN terms. This freezing happens because the system becomes progressively more adiabatic and the individual spin-orbit angles, θ_1 and θ_2 , become locked near a constant value. This also causes the angles Θ_1 and Θ_2 to change rapidly towards the end of the integration as illustrated by the large oscillations of $\cos \Theta_1$ near merger for the systems in the upper panels of Figure 2. We therefore expect that for $\tau_{\text{rp}} \lesssim \tau_{\text{m}}$, the distribution of χ_{eff} of merging BH binaries will also peak near zero. This prediction is confirmed by the population synthesis model presented below.

B. Population synthesis model

We evolved massive stellar triples to BH triples using a modified form of the Binary Stellar Evolution (BSE) package [29] (our prescriptions for mass-loss and stellar winds are identical to those in [30], and include the latest prescriptions for the pulsational pair-instability in massive stars [31]). The tertiary star was evolved simultaneously using the single stellar evolution subset of BSE. We employed 11 different stellar metallicities,

logarithmically-spaced from $1.5Z_\odot$ to $0.01Z_\odot$. We sampled the primary star mass for the inner binary from a Kroupa initial mass function [32] in the range $22 \leq m \leq 150 M_\odot$. The masses of the secondary and tertiary stars were assigned by assuming flat mass ratio (m_2/m_1 and $m_3/(m_1 + m_2)$) distributions between 0 and 1. We take $N \propto \log(P_1/\text{days})^{-0.55}$ for the inner orbital period, and take the outer orbital periods to be flat in log-space (with $a_2 \leq 10^5 \text{AU}$). Orbital eccentricities were drawn from a thermal distribution ($N \propto e$), and the orbital angles from isotropic distributions. Our choice of orbital parameters and masses are consistent with observations of nearby young clusters and associations [e.g., 33]. During the main-sequence evolution we followed the changes to the initial orbital properties due to the mass loss and supernova kicks (based on [34]) experienced by each component of the triple during the formation of a BH [e.g., 35]. We reject any systems for which either the inner or outer binaries collide or in which the triple becomes secularly unstable at any point [36]. Finally, we assume that the spin vectors of the BHs at the time of their formation are aligned with the stellar progenitor spins, and that these progenitor spins are initially aligned with \hat{j} . We set $\chi_1 = \chi_2 = 1$.

After generating initial conditions for the BH triples, we integrated them forward in time until the binary peak GW frequency became larger than 10Hz, up to a maximum time of 13.8Gyr. The right panel of Figure 3 shows the distribution of χ_{eff} for BH binary mergers produced by the LK mechanism in our simulations (which we define to be those that would not have merged if evolved as isolated binaries). This distribution is peaked around zero (with $|\chi_{\text{eff}}| < 0.5(0.25)$ for $\sim 70\%(40\%)$ of sources) and is significantly different from the distribution obtained when ignoring spin precession. The value of χ_{eff} for the BH binaries detected by Advanced LIGO and VIRGO are also displayed in the figure, showing that they are clustered in the range of values $|\chi_{\text{eff}}| \lesssim 0.5$ near the peak of our synthetic distribution.

In the left panel of Figure 3 we plot the value of χ_{eff} as a function of the ratio between the timescale at which the binary enters the LIGO band, τ_{m} , and the value of τ_{rp} at the start of the integration. As predicted, most merging binaries with $\tau_{\text{m}}/\tau_{\text{rp}} \gtrsim 1$ have $\chi_{\text{eff}} \approx 0$, further supporting our interpretation that the peak near zero of the distribution of χ_{eff} is due to the relative precession of the spin vectors as described above.

IV. CONCLUSIONS

For BH binary mergers produced from isolated field binaries, it is expected that the individual BH spins should be nearly aligned with the binary angular momentum [14]. In these standard population synthesis models, the relatively small χ_{eff} of the BH binaries detected so far by LIGO/VIRGO [9–11] is more easily explained if the spin magnitudes were small. This, however, appears to be in

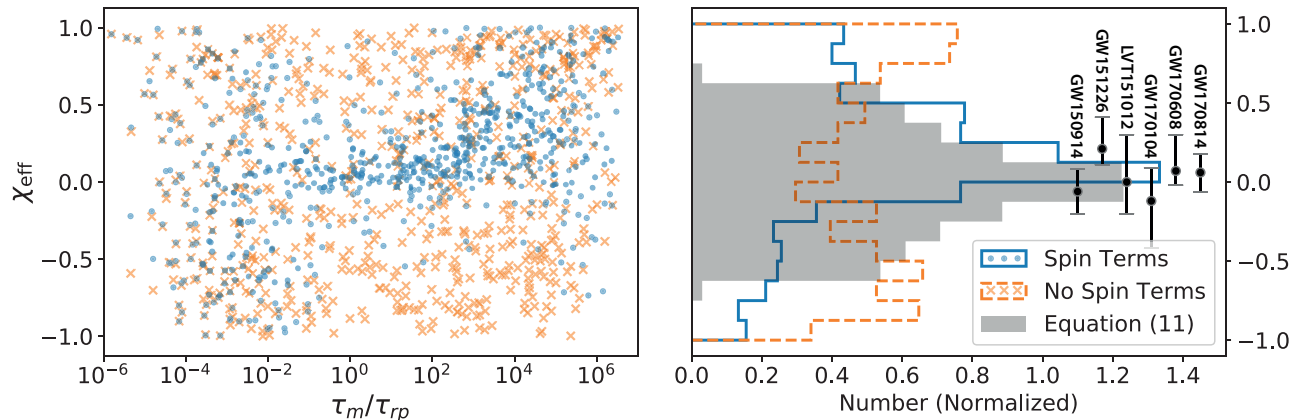


FIG. 3. Distribution of final χ_{eff} for binaries with maximal BH spins that merge due to the LK mechanism in our model. The left panel shows the value of χ_{eff} as a function of the ratio of the initial differential spin precession timescale (τ_{rp}) to the timescale at which the binary enters the LIGO band in our simulations (t_m). Note the clustering of points near $\chi_{\text{eff}} \approx 0$ for $\tau_m/\tau_{\text{rp}} \gtrsim 1$ when the spin-orbit terms (Eq. 2-3) are included (blue filled circles). The right panel shows the distribution of χ_{eff} with the inclusion of spin terms (solid blue) and with no spin terms (dashed orange). Black filled circles give the effective spin parameters of the BH binaries detected by Advanced LIGO/Virgo.

tension with current observational constraints and theoretical models which favor high spins for BHs at birth [16, 17]. If the observed mergers were produced in triple systems instead, we find a more natural and consistent explanation for the low χ_{eff} values measured by LIGO (see Figure 3). Future work will explore how to discriminate between field binaries, field triples, and dynamically-formed binaries [e.g., 37], each of which predicts distinct χ_{eff} distributions. The unique distribution of spin-orbit alignments of such binaries demonstrated in this letter will make their future identification possible as more detections are made by LIGO and other ground-based interferometers.

ACKNOWLEDGMENTS

FA acknowledges support from a CIERA postdoctoral fellowship at Northwestern University. CR acknowledges support from a Pappalardo postdoctoral fellowship at MIT. CP acknowledges support from the Jeffrey L. Bishop Fellowship and from the Gruber Foundation Fellowship. CF acknowledges support from a Sir Edward Youde Memorial Fund scholarship and the Undergraduate Research Opportunities Program at MIT. FA and CR acknowledge the hospitality and support of the Aspen Center for Physics while this work was initiated.

-
- [1] C. L. Rodriguez, M. Zevin, C. Pankow, V. Kalogera, and F. A. Rasio, *ApJL* (2016), 10.3847/2041-8205/832/1/L2.
- [2] B. Farr, D. E. Holz, and W. M. Farr, *ArXiv e-prints* (2017), arXiv:1709.07896 [astro-ph.HE].
- [3] W. M. Farr, S. Stevenson, M. C. Miller, I. Mandel, B. Farr, and A. Vecchio, *Nature* **548**, 426 (2017), arXiv:1706.01385 [astro-ph.HE].
- [4] Y. Kozai, *AJ* **67**, 591 (1962).
- [5] M. L. Lidov, *PLANSS* **9**, 719 (1962).
- [6] F. Antonini, N. Murray, and S. Mikkola, *The Astrophysical Journal* **781**, 45 (2014).
- [7] K. Silsbee and S. Tremaine, *ApJ* **836**, 39 (2017), arXiv:1608.07642 [astro-ph.HE].
- [8] F. Antonini, S. Toonen, and A. S. Hamers, *ApJ* **841**, 77 (2017), arXiv:1703.06614.
- [9] B. P. Abbott, R. Abbott, T. D. Abbott, M. R. Abernathy, F. Acernese, K. Ackley, C. Adams, T. Adams, P. Addesso, R. X. Adhikari, and et al., *Physical Review Letters* **116**, 241102 (2016), arXiv:1602.03840 [gr-qc].
- [10] B. P. Abbott, R. Abbott, T. D. Abbott, M. R. Abernathy, F. Acernese, K. Ackley, C. Adams, T. Adams, P. Addesso, R. X. Adhikari, and et al., *Physical Review X* **6**, 041015 (2016), arXiv:1606.04856 [gr-qc].
- [11] B. P. Abbott, R. Abbott, T. D. Abbott, F. Acernese, K. Ackley, C. Adams, T. Adams, P. Addesso, R. X. Adhikari, V. B. Adya, and et al., *Physical Review Letters* **119**, 141101 (2017), arXiv:1709.09660 [gr-qc].
- [12] B. P. Abbott, R. Abbott, T. D. Abbott, F. Acernese, K. Ackley, C. Adams, T. Adams, P. Addesso, R. X. Adhikari, V. B. Adya, and et al., *Physical Review Letters* **118**, 221101 (2017), arXiv:1706.01812 [gr-qc].
- [13] B. P. Abbott, R. Abbott, T. D. Abbott, F. Acernese, K. Ackley, C. Adams, T. Adams, P. Addesso, R. X. Adhikari, V. B. Adya, and et al., (2017), arXiv:1711.05578 [gr-qc].
- [14] V. Kalogera, *The Astrophysical Journal* **541**, 319 (2000).
- [15] K. Belczynski, J. Klencki, G. Meynet, C. L. Fryer, D. A. Brown, M. Chruslinska, W. Gladysz, R. O’Shaughnessy,

- T. Bulik, E. Berti, D. E. Holz, D. Gerosa, M. Giersz, S. Ekstrom, C. Georgy, A. Askar, J.-P. Lasota, and D. Wysocki, ArXiv e-prints (2017), arXiv:1706.07053 [astro-ph.HE].
- [16] C. F. Gammie, S. L. Shapiro, and J. C. McKinney, *ApJ* **602**, 312 (2004), astro-ph/0310886.
- [17] J. M. Miller, M. C. Miller, and C. S. Reynolds, *ApJL* **731**, L5 (2011), arXiv:1102.1500 [astro-ph.HE].
- [18] A. Hale, *AJ* **107**, 306 (1994).
- [19] E. Corsaro, Y.-N. Lee, R. A. García, P. Hennebelle, S. Mathur, P. G. Beck, S. Mathis, D. Stello, and J. Bouvier, *Nature Astronomy* **1**, 0064 (2017), arXiv:1703.05588 [astro-ph.SR].
- [20] B. Liu, D. J. Muñoz, and D. Lai, *MNRAS* **447**, 747 (2015), arXiv:1409.6717 [astro-ph.EP].
- [21] C. Petrovich, *ApJ* **799**, 27 (2015), arXiv:1405.0280 [astro-ph.EP].
- [22] J. M. O. Antognini, *MNRAS* **452**, 3610 (2015), arXiv:1504.05957 [astro-ph.EP].
- [23] O. Blaes, M. H. Lee, and A. Socrates, *The Astrophysical Journal* **578**, 775 (2002).
- [24] J. D. Schnittman, *Physical Review D - Particles, Fields, Gravitation and Cosmology* **70** (2004), 10.1103/PhysRevD.70.124020.
- [25] T. Apostolatos, C. Cutler, G. Sussman, and K. Thorne, *Physical Review D* **49**, 6274 (1994).
- [26] N. I. Storch, K. R. Anderson, and D. Lai, *Science* **345**, 1317 (2014).
- [27] N. I. Storch and D. Lai, *Monthly Notices of the Royal Astronomical Society* **448**, 1821 (2015).
- [28] B. Liu and D. Lai, *ApJL* **846**, L11 (2017), arXiv:1706.02309 [astro-ph.HE].
- [29] J. R. Hurley, C. A. Tout, and O. R. Pols, *Monthly Notices of the Royal Astronomical Society* **329**, 897 (2002).
- [30] C. L. Rodriguez, S. Chatterjee, and F. A. Rasio, *Physical Review D* **93**, 084029 (2016).
- [31] K. Belczynski, A. Heger, W. Gladysz, A. J. Ruiter, S. Woosley, G. Wiktorowicz, H.-Y. Chen, T. Bulik, R. O’Shaughnessy, D. E. Holz, C. L. Fryer, and E. Berti, *A&A* **594**, A97 (2016), arXiv:1607.03116 [astro-ph.HE].
- [32] P. Kroupa and C. Weidner, *The Astrophysical Journal* **598**, 1076 (2003).
- [33] H. Sana, S. E. de Mink, A. de Koter, N. Langer, C. J. Evans, M. Gieles, E. Gosset, R. G. Izzard, J.-B. Le Bouquin, and F. R. N. Schneider, *Science (New York, N.Y.)* **337**, 444 (2012).
- [34] C. L. Fryer, K. Belczynski, G. Wiktorowicz, M. Dominik, V. Kalogera, and D. E. Holz, *The Astrophysical Journal* **749**, 91 (2012).
- [35] S. Toonen, A. Hamers, and S. Portegies Zwart, *Computational Astrophysics and Cosmology* **3**, 6 (2016), arXiv:1612.06172 [astro-ph.SR].
- [36] R. A. Mardling and S. J. Aarseth, *MNRAS* **321**, 398 (2001).
- [37] C. L. Rodriguez, C.-J. Haster, S. Chatterjee, V. Kalogera, and F. A. Rasio, *The Astrophysical Journal* **824**, L8 (2016).